



# Thermal properties and crystallization of BaO–MoO<sub>3</sub>–P<sub>2</sub>O<sub>5</sub> glasses

Petr Kalenda<sup>1</sup> · Ladislav Koudelka<sup>1</sup> · Petr Mošner<sup>1</sup> · Ludvík Beneš<sup>2</sup> · Zdeněk Černošek<sup>1</sup>

Received: 10 July 2017 / Accepted: 28 November 2017 / Published online: 4 December 2017  
© Akadémiai Kiadó, Budapest, Hungary 2017

## Abstract

The thermal behavior and crystallization of barium molybdate-phosphate glasses were studied in two compositional series, namely A: (100 – x)Ba(PO<sub>3</sub>)<sub>2</sub>–xMoO<sub>3</sub> (with x = 0–70 mol%) and B: 50BaO–yMoO<sub>3</sub>–(50 – y)P<sub>2</sub>O<sub>5</sub> (with y = 0–15 mol% MoO<sub>3</sub>). Thermal properties were studied with differential thermal analysis and dilatometry. Glass transition temperature increases in series A in the range of 0–40 mol% MoO<sub>3</sub> and then decreases with a further increase in MoO<sub>3</sub> content, whereas the thermal expansion coefficient in series A reveals a minimum at 50 mol% MoO<sub>3</sub>. These trends are not observed in series B, where the glass transition temperature increases in the range of 0–15 mol% MoO<sub>3</sub> and the thermal expansion coefficient almost does not change. Crystallization of these glasses was studied by X-ray diffraction analysis, Raman and <sup>31</sup>P MAS NMR spectroscopy. Large thermal stability of glass with a composition 35BaO–30MoO<sub>3</sub>–35P<sub>2</sub>O<sub>5</sub> toward crystallization was demonstrated. Crystallization of glasses resulted in the formation of the compound Ba(MoO<sub>2</sub>)<sub>2</sub>(PO<sub>4</sub>)<sub>2</sub> in this ternary system. Raman spectroscopy also provided information on the formation of glass-crystalline samples in some studied compositions.

**Keywords** Barium molybdate-phosphate glasses · Thermal analysis · Crystallization · XRD · Raman spectra

## Introduction

The unique properties of phosphate-based glasses, such as low melting temperature, low glass transition temperature, high transparency for ultraviolet (UV) light, low dispersion and relatively high refractive indices, compared to silicate-based glasses make them attractive for various technological applications, such as hermetic seals, organic/inorganic composites, biomaterials, solid-state electrolytes or materials for immobilization of nuclear waste [1, 2]. Special attention is paid to phosphate materials modified with transitional-metal (TM) oxides, such as Nb<sub>2</sub>O<sub>5</sub>, WO<sub>3</sub> or MoO<sub>3</sub> [3–5], due to the fact that the high electrostatic field strength ( $z/a^2$ ) of P<sup>5+</sup> allows incorporating a high amount of TM oxides in phosphate glasses, again in comparison

with silicate glasses [1]. A lot of attention is also paid to investigation of crystallization processes and crystallization mechanisms in phosphate glasses [6, 7].

The structure of NaPO<sub>3</sub>–MoO<sub>3</sub> glasses was studied with solid-state nuclear magnetic resonance and Raman spectroscopy by Santagneli et al. [4], who suggested that the majority of molybdenum species are four-coordinated; however, MAS NMR experiments show also the presence of some six-coordinate molybdenum. The redox behavior of these glasses was studied in [8] where the authors Poirier et al. from the results of XANES spectra concluded that only MoO<sub>6</sub> octahedra are present in the NaPO<sub>3</sub>–MoO<sub>3</sub> glass structure. Structural study of PbO–MoO<sub>3</sub>–P<sub>2</sub>O<sub>5</sub> glasses was reported in [9]. Study of the thermal properties of these glasses and their crystallization [10] showed on the formation of the crystalline compound at the glass composition 25PbO·50MoO<sub>3</sub>·25P<sub>2</sub>O<sub>5</sub>, which corresponded to the formula Pb(MoO<sub>2</sub>)<sub>2</sub>(PO<sub>4</sub>)<sub>2</sub>. Its structure was determined by Masse et al. [11], who found that MoO<sub>6</sub> octahedra and PO<sub>4</sub> tetrahedra are basic structural units in this compound.

We have recently studied glass formation in the ternary system BaO–MoO<sub>3</sub>–P<sub>2</sub>O<sub>5</sub> [12] and determined the glass-forming region in this system, which covers glasses with

✉ Ladislav Koudelka  
ladislav.koudelka@upce.cz

<sup>1</sup> Department of General and Inorganic Chemistry, Faculty of Chemical Technology, University of Pardubice, 532 10 Pardubice, Czech Republic

<sup>2</sup> Joint Laboratory of Solid State Chemistry of the Institute of Macromolecular Chemistry of Academy of Sciences, v.v.i., University of Pardubice, 532 10 Pardubice, Czech Republic

the MoO<sub>3</sub> content 0–70 mol% and also a glassy sample with only 10 mol% P<sub>2</sub>O<sub>5</sub>.

The aim of the present work was the investigation of thermal properties of BaO–MoO<sub>3</sub>–P<sub>2</sub>O<sub>5</sub> glasses in two compositional series, starting from barium metaphosphate Ba(PO<sub>3</sub>)<sub>2</sub>: series A: (100 – *x*)Ba(PO<sub>3</sub>)<sub>2</sub>–*x*MoO<sub>3</sub> (with *x* = 0–70 mol%) and B: 50BaO–*y*MoO<sub>3</sub>–(50 – *y*)P<sub>2</sub>O<sub>5</sub> (with *y* = 0–15 mol% MoO<sub>3</sub>). We also studied the crystallization process in these glasses, and crystalline products, obtained by annealing glass powders, were analyzed by X-ray diffraction and Raman spectroscopy.

## Experimental

Glasses of the BaO–MoO<sub>3</sub>–P<sub>2</sub>O<sub>5</sub> system were prepared by melting analytical grade BaCO<sub>3</sub>, MoO<sub>3</sub> and H<sub>3</sub>PO<sub>4</sub>, using a total batch weight of 30 g. The homogenized starting mixtures were slowly calcined up to 600 °C and held at this temperature for 2 h in order to remove water. The reaction mixtures were then melted at a temperature range 900–1200 °C under ambient air, in a platinum crucible. The melt was subsequently poured into a preheated graphite mold and the obtained glasses were then cooled to room temperature. Weight loss measurements indicated that the volatilization losses were not significant, even at the highest temperature, and hence the batch compositions can be considered as reflecting actual compositions. Glass composition was also checked by XRF, and the results of EDAX analysis of glasses are given in Table 1. The

**Table 1** Composition of BaO–MoO<sub>3</sub>–P<sub>2</sub>O<sub>5</sub> glasses

Series	Composition (mol%)					
	Batch			Analyzed (EDAX)		
	BaO	MoO <sub>3</sub>	P <sub>2</sub> O <sub>5</sub>	BaO	MoO <sub>3</sub>	P <sub>2</sub> O <sub>5</sub>
A	50	0	50	50.1	0	49.9
	47.5	5	47.5	47.6	4.9	47.5
	45	10	45	45.0	10.0	45.0
	42.5	15	42.5	42.7	14.9	42.4
	40	20	40	39.9	20.0	40.1
	35	30	35	35.3	29.8	34.9
	30	40	30	30.1	39.9	30.0
	25	50	25	25.0	50.0	25.0
	20	60	20	20.2	59.8	20.0
	15	70	15	15.1	69.8	15.1
B	50	0	50	50.1	0	49.9
	50	5	45	50.1	5.0	44.9
	50	10	40	50.0	9.9	40.1
	50	15	35	50.2	14.7	35.1

amorphous character of the prepared glasses was checked by X-ray diffraction analysis.

The corresponding polycrystalline samples were prepared by annealing glass powder samples in a platinum crucible for 3 h at the temperatures above the crystallization peaks determined from DTA measurements. Identification of the obtained products was carried out by X-ray diffraction analysis.

Thermal behavior of the glasses was studied with the DTA 404 PC (Netzsch) operating in the heat flux DSC mode at a heating rate of 10 °C min<sup>−1</sup> over the temperature range 30–1000 °C. The measurements were taken with 60 mg powder samples (average particle size was 10 μm) in a silica crucible under an inert atmosphere of N<sub>2</sub>. The empty silica crucible was used as a reference material. The DTA equipment was calibrated using RbNO<sub>3</sub>, Ag<sub>2</sub>SO<sub>4</sub>, K<sub>2</sub>CrO<sub>4</sub> and BaCO<sub>3</sub> for the temperature range 100–900 °C; heating rate of 10 °C min<sup>−1</sup> was used for calibration as well as for the measurements.

The thermal expansion coefficient,  $\alpha$ , the glass transition temperature,  $T_g$ , and the dilatometric softening temperature,  $T_d$ , were measured on bulk samples with dimensions of 20 × 5 × 5 mm using a dilatometer DIL 402 PC (Netzsch). From the obtained dilatometric curves, the coefficient of thermal expansion,  $\alpha$ , was determined as the mean value in the temperature range of 100–200 °C, the glass transition temperature,  $T_g$ , was determined from the change in the slope of the elongation versus temperature plot, and dilatometric softening temperature,  $T_d$ , was determined as the maximum of the expansion trace corresponding to the onset of viscous deformation. The dilatometric measurements were taken in the air at a heating rate of 5 °C min<sup>−1</sup>.

A Bruker D8 Advance diffractometer with CuK $\alpha$  radiation was used for the identification of crystalline phases. A database of inorganic compounds from International Center of Diffraction Data [13] was used for the phase identification.

The Raman spectra in the range 1400–200 cm<sup>−1</sup> were measured on bulk and powder samples at room temperature using a Horiba–Jobin–Yvon LaBRam HR spectrometer. The spectra were recorded in back-scattering geometry under excitation with Nd:YAG laser radiation (532 nm) at a power of 12 mW on the sample. The spectral slit width was 1.5 cm<sup>−1</sup> and the total integration time was 50 s.

<sup>31</sup>P MAS NMR spectra were measured at 9.4 T on a BRUKER Avance 400 spectrometer with a 4 mm probe. The spinning speed was 12.5 kHz and relaxation (recycling) delay was 180 s. The chemical shifts of <sup>31</sup>P nuclei are given relative to H<sub>3</sub>PO<sub>4</sub> at 0 ppm.

Glass density,  $\rho$ , was determined with bulk samples with the Archimedes method, using toluene as the immersion liquid. Crystal density,  $\rho$ , was determined using helium gas

pycnometer AccuPyc II 1340, where the volume of the sample is measured by measuring volume of the helium gas which is displaced by the sample.

## Results and discussion

### Thermal properties of glasses

We have prepared 13 glass samples of the BaO–MoO<sub>3</sub>–P<sub>2</sub>O<sub>5</sub> ternary system by the procedure described above. Their composition is shown in Table 1. In order to investigate the effect of composition on the thermal properties and crystallization of these glasses, we have studied glasses in two compositional series A:  $(100 - x)\text{Ba}(\text{PO}_3)_2 - x\text{MoO}_3$  with  $x = 0-70$  mol% MoO<sub>3</sub> and B:  $50\text{BaO} - y\text{MoO}_3 - (50 - y)\text{P}_2\text{O}_5$  with  $y = 0-15$  mol% MoO<sub>3</sub>.

DTA curves of the glass series A:  $(100 - x)\text{Ba}(\text{PO}_3)_2 - x\text{MoO}_3$  and B:  $50\text{BaO} - y\text{MoO}_3 - (50 - y)\text{P}_2\text{O}_5$  are shown in Figs. 1 and 2. As can be seen from these figures, glasses of the series A and B, with the exception of the glass with  $x = 30$  in compositional series A:  $(100 - x)\text{Ba}(\text{PO}_3)_2 - x\text{MoO}_3$ , reveal pronounced crystallization peaks. In the high-temperature region, we can also see endothermic peaks corresponding to the melting of the corresponding crystalline phases. The crystallization temperature was

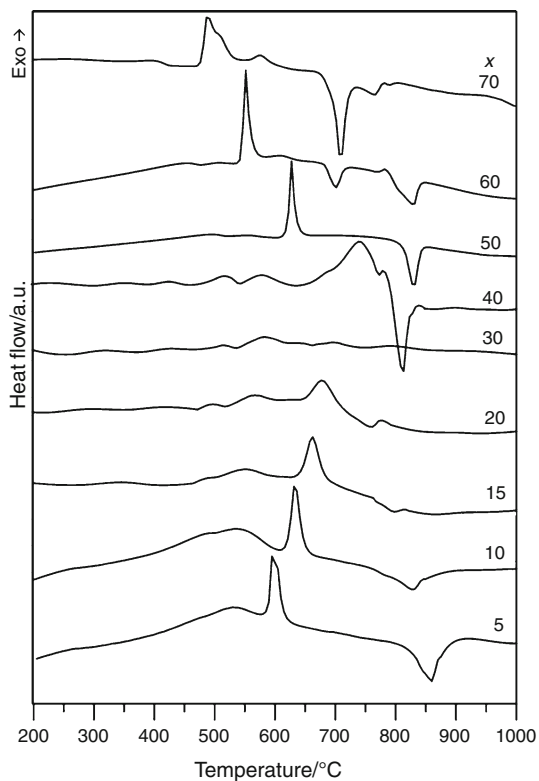


Fig. 1 DTA curves of the glass series A:  $(100 - x)\text{Ba}(\text{PO}_3)_2 - x\text{MoO}_3$

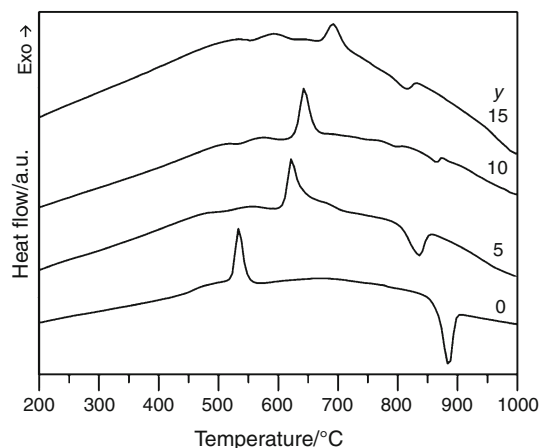


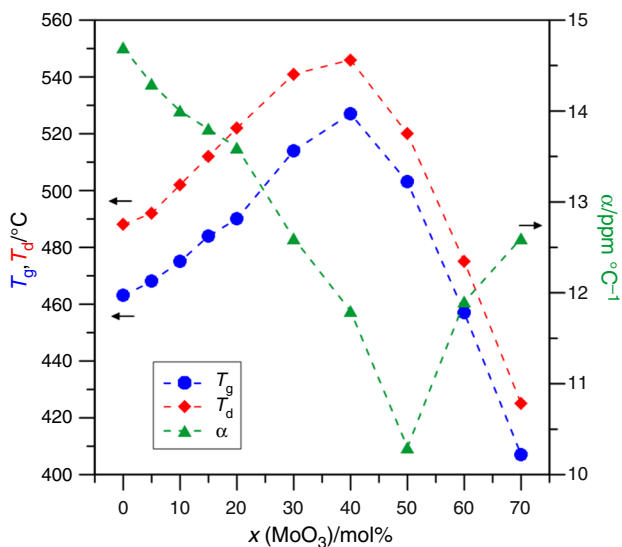
Fig. 2 DTA curves of the glass series B:  $50\text{BaO} - y\text{MoO}_3 - (50 - y)\text{P}_2\text{O}_5$

determined from these curves as the onset of the crystallization peak and the obtained values are given in Table 2. As can be seen also from Fig. 1, glass with the composition  $35\text{BaO} - 30\text{MoO}_3 - 35\text{P}_2\text{O}_5$  did not crystallize even after 24 h annealing, due to its extraordinary thermal stability against crystallization. This fact corresponds well with the compositional dependence of the thermal stability of the studied glasses, evaluated as a simple difference between crystallization temperature  $T_c$  and glass transition temperature  $T_g$ . The values of the difference  $(T_c - T_g)$  given in Table 2 show a gradual increase in this difference in glass series A from  $x = 0$  to  $x = 30$  and is followed by a steady decrease in the range  $x = 40-70$  mol% MoO<sub>3</sub>. Basic thermoanalytical data of the prepared glasses—glass transition temperature,  $T_g$ , dilatometric softening temperature  $T_d$ , coefficient of thermal expansion,  $\alpha$ , crystallization temperature,  $T_c$ , and the difference  $(T_c - T_g)$ —are given in Table 2. The tabulated values of  $T_g$  were obtained from dilatometric measurements.

The compositional dependence of the glass transition temperature,  $T_g$ , dilatometric softening temperature,  $T_d$ , and coefficient of thermal expansion,  $\alpha$ , of glasses in the compositional series A:  $(100 - x)\text{Ba}(\text{PO}_3)_2 - x\text{MoO}_3$ , obtained from dilatometric measurements, are also shown in Fig. 3. In this series, the glass transition temperature at first increases from 463 °C, for the starting barium metaphosphate glass, up to 527 °C for the glass with 40 mol% of MoO<sub>3</sub>. Subsequently, from  $x = 40$  to  $x = 70$ ,  $T_g$  values decrease down to 407 °C for the glass with 70 mol% MoO<sub>3</sub>. A similar trend was also observed for the dilatometric softening temperature. The coefficient of thermal expansion reveals the opposite trend, because at first it decreases from 14.7 ppm °C<sup>-1</sup> down to 10.3 ppm °C<sup>-1</sup> within the concentration range  $x = 0-50$  mol% MoO<sub>3</sub> and then increases back up to 12.6 ppm °C<sup>-1</sup> for the glass with  $x = 70$ .

**Table 2** Composition, glass transition temperature  $T_g$ , dilatometric softening temperature  $T_d$  and thermal expansion coefficient,  $\alpha$ , crystallization temperature,  $T_c$ , and criterion of thermal stability of glasses,  $T_c - T_g$ , of BaO–MoO<sub>3</sub>–P<sub>2</sub>O<sub>5</sub> glasses

Series	BaO/mol%	MoO <sub>3</sub> /mol%	P <sub>2</sub> O <sub>5</sub> /mol%	$T_g \pm 2/^\circ\text{C}$	$T_d \pm 2/^\circ\text{C}$	$\alpha \pm 0.3$ (100–200 °C)/ppm °C <sup>-1</sup>	$T_c \pm 2/^\circ\text{C}$	$T_c - T_g$
A	50	0	50	463	488	14.7	523	60
	47.5	5	47.5	468	492	14.3	592	124
	45	10	45	475	502	14.0	622	147
	42.5	15	42.5	484	512	13.8	644	160
	40	20	40	490	522	13.6	652	162
	35	30	35	514	541	12.6	–	–
	30	40	30	527	546	11.8	704	177
	25	50	25	503	520	10.3	622	119
	20	60	20	457	475	11.9	546	89
	15	70	15	407	425	12.6	479	72
B	50	0	50	463	488	14.7	523	60
	50	5	45	496	516	14.9	610	114
	50	10	40	517	536	15.2	630	113
	50	15	35	538	558	14.5	674	116

**Fig. 3** Compositional dependence of glass transition temperature,  $T_g$ , dilatometric softening temperature,  $T_d$  and the coefficient of thermal expansion in the glass series A:  $(100 - x)\text{Ba}(\text{PO}_3)_2 - x\text{MoO}_3$  on the MoO<sub>3</sub> content. The error in the values of  $T_g$  and  $T_d$  is smaller than the symbol size. The lines are only a guide to the eye

Generally,  $T_g$  of oxide glasses increases with the increasing bond strength, cross-link density and closeness of packing of the glass. Since the energy of Mo–O bonds ( $E_{\text{Mo-O}} = 560.2 \pm 20.9 \text{ kJ mol}^{-1}$  [14]) is weaker than the energy of P–O bonds ( $E_{\text{P-O}} = 599.1 \pm 12.6 \text{ kJ mol}^{-1}$  [14]) and comparable with the energy of Ba–O bonds ( $E_{\text{Ba-O}} = 561.9 \pm 13.4 \text{ kJ mol}^{-1}$  [14]), the mean bond strength actually decreases with an increase in MoO<sub>3</sub> content. Therefore, the main factors, influencing the observed increase in  $T_g$  in the first glass series, are increasing cross-link density and

closeness of packing of the glass within the range  $x = 0$ –40. Consequently, we can assume that the structural network of glasses in the first series has an optimum cross-linking density at  $x = 40$ . In the following part of the compositional dependence of  $T_g$  (from  $x = 40$  to  $x = 70$ ), the replacement of stronger P–O bonds by weaker Mo–O bonds plays a decisive role. A similar maximum on the compositional dependence of phosphate glasses with MoO<sub>3</sub> was also observed in the NaPO<sub>3</sub>–MoO<sub>3</sub> compositional line [4] or in the PbO–MoO<sub>3</sub>–P<sub>2</sub>O<sub>5</sub> glasses [10].

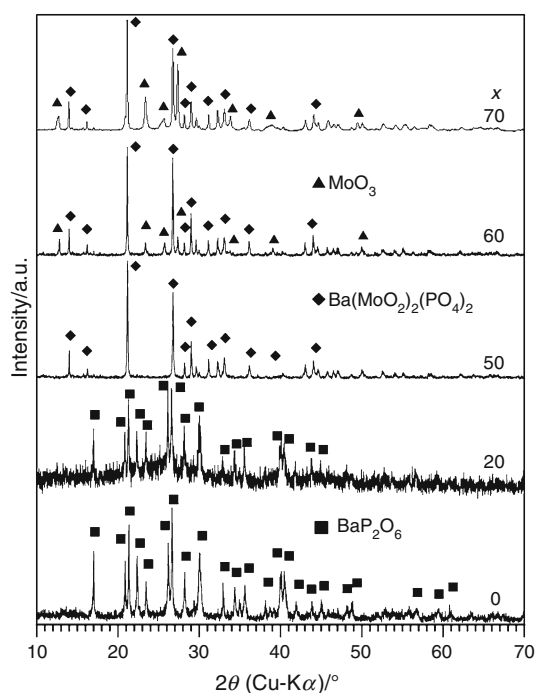
In the compositional series  $50\text{BaO} - y\text{MoO}_3 - (50 - y)\text{P}_2\text{O}_5$ , the values of  $T_g$  and  $T_d$  monotonously increase with increasing MoO<sub>3</sub> content (see Table 2) within the range  $y = 0$ –15 mol% MoO<sub>3</sub>, since the glass-forming region here is narrower in comparison with glass series A. The values of the coefficient of thermal expansion  $\alpha$  almost do not change significantly.

## Glass crystallization

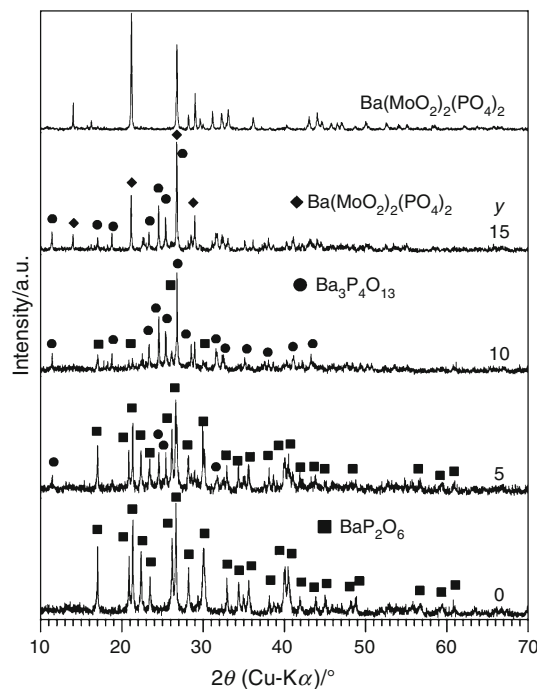
Crystallization products were obtained by annealing glass powders for 3 h at temperatures above their crystallization peaks on the DTA curve. The annealing temperatures are provided in Table 3 along with the compositions of the crystalline products identified by X-ray diffraction analysis and the application of database PDF-4 [13]. The diffraction patterns of the crystalline phases formed from glasses of the series A and B are given in Figs. 4 and 5. Four crystalline phases were found, three were identified in compositional series A and three in compositional series B. Crystalline compounds BaP<sub>2</sub>O<sub>6</sub> and Ba(MoO<sub>2</sub>)<sub>2</sub>(PO<sub>4</sub>)<sub>2</sub> are present in both compositional series (see Table 3). Crystalline barium metaphosphate BaP<sub>2</sub>O<sub>6</sub> (could be written

**Table 3** Annealing temperatures,  $T_a$ , and crystallization products of BaO–MoO<sub>3</sub>–P<sub>2</sub>O<sub>5</sub> glasses

Series	BaO/mol%	MoO <sub>3</sub> /mol%	P <sub>2</sub> O <sub>5</sub> /mol%	$T_a/^\circ\text{C}$	Products of crystallization
A	50	0	50	600	BaP <sub>2</sub> O <sub>6</sub>
	47.5	5	47.5	650	BaP <sub>2</sub> O <sub>6</sub>
	45	10	45	680	BaP <sub>2</sub> O <sub>6</sub>
	42.5	15	42.5	700	BaP <sub>2</sub> O <sub>6</sub>
	40	20	40	600	BaP <sub>2</sub> O <sub>6</sub>
	35	30	35	600	–
	30	40	30	600	Ba(MoO <sub>2</sub> ) <sub>2</sub> (PO <sub>4</sub> ) <sub>2</sub>
	25	50	25	650/680	Ba(MoO <sub>2</sub> ) <sub>2</sub> (PO <sub>4</sub> ) <sub>2</sub> , MoO <sub>3</sub>
	20	60	20	600	Ba(MoO <sub>2</sub> ) <sub>2</sub> (PO <sub>4</sub> ) <sub>2</sub> , MoO <sub>3</sub>
	15	70	15	550	Ba(MoO <sub>2</sub> ) <sub>2</sub> (PO <sub>4</sub> ) <sub>2</sub>
B	50	0	50	600	BaP <sub>2</sub> O <sub>6</sub>
	50	5	45	700	BaP <sub>2</sub> O <sub>6</sub> , Ba <sub>3</sub> P <sub>4</sub> O <sub>13</sub>
	50	10	40	700	Ba <sub>3</sub> P <sub>4</sub> O <sub>13</sub> , BaP <sub>2</sub> O <sub>6</sub>
	50	15	35	700	Ba <sub>3</sub> P <sub>4</sub> O <sub>13</sub> , Ba(MoO <sub>2</sub> ) <sub>2</sub> (PO <sub>4</sub> ) <sub>2</sub>

**Fig. 4** XRD patterns of crystallized samples of the glass series A:  $(100 - x)\text{Ba}(\text{PO}_3)_2 - x\text{MoO}_3$ 

also as  $\text{Ba}(\text{PO}_3)_2$  was found in crystallization products of the series A with  $x = 0$ – $20$ . Glass with  $x = 30$  was extraordinarily thermally stable and did not crystallize even after annealing the powdered glass for 24 h. In series A, we expected for the sample with  $x = 50$  a compound with the formula  $\text{Ba}(\text{MoO}_2)_2(\text{PO}_4)_2$  as a crystallization product, as reported by Masse et al. [11] in 1985. Nevertheless, the X-ray diffraction pattern of our annealed sample with  $x = 50$  was different from that reported by

**Fig. 5** XRD patterns of crystallized samples of the glass series B:  $50\text{BaO} - y\text{MoO}_3 - (50 - y)\text{P}_2\text{O}_5$ 

Masse et al. [11]. The obtained diffractogram from our sample (63 sharp diffraction lines with FWHM of approximately  $0.07^\circ 2\Theta$ ) suggests a monoclinic cell of dimensions  $a = 13.8600(2) \text{ \AA}$ ,  $b = 12.3207(2) \text{ \AA}$ ,  $c = 6.3529(1) \text{ \AA}$  and  $\beta = 120.86(1)^\circ$ , with figures of merit  $M(20) = 36.4$  [15] and  $F(20) = 63.3$  (0.0052, 61) [16],  $I/I_{\text{cor}} = 3.4$ . A possible space group  $\text{P}2_1/n$  was found using the CHECKCELL program [17]. The volume of the unit cell is  $931.3(4) \text{ \AA}^3$ , and we assume that the unit cell



contains four formula units of  $\text{Ba}(\text{MoO}_2)_2(\text{PO}_4)_2$  ( $M = 583.15$ ,  $Z = 4$ ). In this case, the calculated density of the crystalline compound  $D_x = 4.159 \text{ g cm}^{-3}$  is in good agreement with the experimental value of  $4.034 \text{ g cm}^{-3}$  for crystallized glass of the same composition.

A possible explanation for the disagreement between the diffraction patterns could be due to the fact that the authors [11] prepared the compound  $\text{Ba}(\text{MoO}_2)_2(\text{PO}_4)_2$  by the reaction of  $\text{Ba}(\text{PO}_3)_2$  with  $\text{MoO}_3$  at  $600^\circ\text{C}$ , so another crystal modification may have occurred in their case. The diffraction lines of the ternary compound  $\text{Ba}(\text{MoO}_2)_2(\text{PO}_4)_2$  were observed also on the diffraction patterns of annealed samples with  $x = 40, 60$  and  $70$  mol%  $\text{MoO}_3$  (see Table 3 and Fig. 4). As can be seen from Table 3, we also found crystalline  $\text{MoO}_3$  on the XRD diagrams of the annealed samples with  $x = 60$  and  $70$ . In the compositional series B:  $50\text{BaO}-y\text{MoO}_3-(50-y)\text{P}_2\text{O}_5$  diffraction lines of barium metaphosphate  $\text{BaP}_2\text{O}_6$  and barium tetrphosphate  $\text{Ba}_3\text{P}_4\text{O}_{13}$  were identified at the annealed samples with  $y = 0-10$  and diffraction lines of  $\text{Ba}(\text{MoO}_2)_2(\text{PO}_4)_2$  at the sample with  $y = 15$ .

Raman spectra of all annealed samples were also obtained. These spectra are shown in Fig. 6 for the compositional series A:  $(100-x)\text{Ba}(\text{PO}_3)_2-x\text{MoO}_3$  and in Fig. 7 for the compositional series B:  $\text{BaO}-y\text{MoO}_3-(50-y)\text{P}_2\text{O}_5$ . Raman spectra show good agreement with the results obtained by X-ray diffraction analysis in terms of identified crystalline phases. However, Raman spectra show also the presence of the glass-crystalline state in some samples. The crystalline phases possess sharp vibrational bands, while non-crystalline glassy phases possess wide vibrational bands. For example, on the Raman

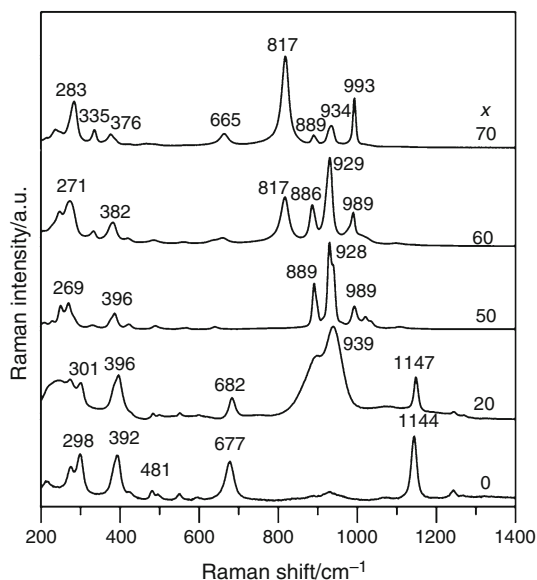


**Fig. 6** Raman spectra of crystallized samples of the glass series A:  $(100-x)\text{Ba}(\text{PO}_3)_2-x\text{MoO}_3$

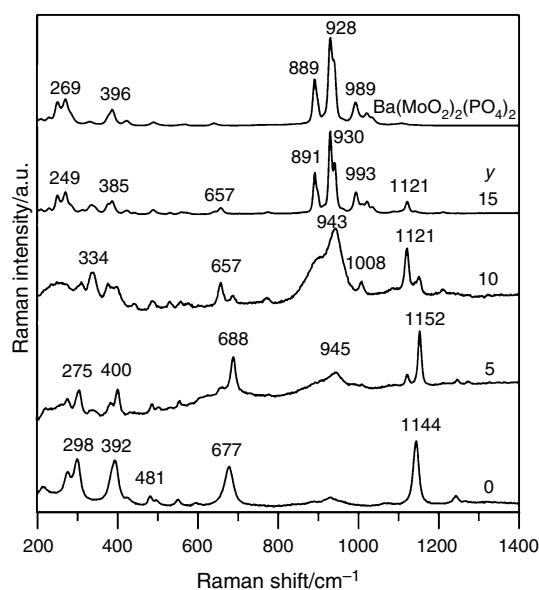


**Fig. 7** Raman spectra of crystallized samples of the glass series B:  $50\text{BaO}-y\text{MoO}_3-(50-y)\text{P}_2\text{O}_5$

spectra of the glass with  $x = 10$  mol%  $\text{MoO}_3$  from compositional series A, sharp vibrational bands of barium metaphosphate at  $1150$  and  $686 \text{ cm}^{-1}$  are present, but the broad bands at  $938$  and  $890 \text{ cm}^{-1}$  show the presence of the remaining glassy phase containing molybdate structural units. On the Raman spectrum of the annealed sample with  $x = 30$  mol%  $\text{MoO}_3$ , no sharp lines of crystalline products are present; i.e., there is only glassy phase in the sample, which confirms its extra thermal stability in agreement with the results of DSC analysis (see Fig. 2). The Raman spectrum of the annealed glass sample with  $x = 50$  mol%  $\text{MoO}_3$  reveals sharp peaks of the crystalline compound  $\text{Ba}(\text{MoO}_2)_2(\text{PO}_4)_2$ . Three dominant vibrational bands are placed in the region  $800-1150 \text{ cm}^{-1}$  at  $889$ ,  $928$  and  $989 \text{ cm}^{-1}$  and another two at  $269$  and  $396 \text{ cm}^{-1}$ . Raman spectra also reveal vibrational bands characteristic of crystalline  $\text{MoO}_3$  at  $817 \text{ cm}^{-1}$  at the samples with  $x = 60$  and  $70$ , which is also in agreement with the X-ray diffraction analysis.

Raman spectra of the annealed samples of the compositional series B  $50\text{BaO}-y\text{MoO}_3-(50-y)\text{P}_2\text{O}_5$  are shown in Fig. 7. Raman spectra of the annealed glasses with  $y = 0-10$  mol%  $\text{MoO}_3$  reveal the presence of crystalline barium phosphates  $\text{BaP}_2\text{O}_6$  and  $\text{Ba}_3\text{P}_4\text{O}_{13}$ . Nevertheless, molybdate structural units remain in a glassy state, as manifested by the presence of the strong vibrational band at  $943 \text{ cm}^{-1}$  with a shoulder on its left side for the glass with  $y = 10$ . In the Raman spectrum of the annealed glass with  $y = 15$  mol%  $\text{MoO}_3$ , vibrational bands of the compound  $\text{Ba}(\text{MoO}_2)_2(\text{PO}_4)_2$  were identified as dominant features of

the Raman spectrum of crystalline products present in the sample.

### Glass to crystal transformation of 25BaO–50MoO<sub>3</sub>–25P<sub>2</sub>O<sub>5</sub> glass

Since a new crystalline compound Ba(MoO<sub>2</sub>)<sub>2</sub>(PO<sub>4</sub>)<sub>2</sub> was identified, more attention was paid to the process of crystallization of the corresponding glass with the composition 25BaO–50MoO<sub>3</sub>–25P<sub>2</sub>O<sub>5</sub> ( $x = 50$  in compositional series A: (100 –  $x$ )Ba(PO<sub>3</sub>)<sub>2</sub>– $x$ MoO<sub>3</sub>). Crystallization and melting of the resulting crystalline phase are well-represented on the DTA curve obtained with the glass sample (Fig. 1). This glass possesses a glass transition temperature  $503 \pm 2$  °C (determined from dilatometric curve) and the beginning of crystallization (onset value in Fig. 1) of 622 °C. The extrapolated value of the onset of the melting peak of the crystalline phase was determined as  $815 \pm 2$  °C. The area of the exothermic crystallization peak is very close to the area of the endothermic melting peak, and so it is a logical assumption that the melting peak could be attributed to the crystalline phase formed in the previous crystallization process.

We also measured the density of the 25BaO–50MoO<sub>3</sub>–25P<sub>2</sub>O<sub>5</sub> glass, which was evaluated as  $3.940 \text{ g cm}^{-3}$ , and the density of crystalline compound Ba(MoO<sub>2</sub>)<sub>2</sub>(PO<sub>4</sub>)<sub>2</sub> with  $4.034 \text{ g cm}^{-3}$ . Obviously, the density of the crystalline samples is higher than the density of the corresponding glasses, which is a classical observation. Accordingly, the molar volume of glass is higher than the molar volume of the corresponding crystalline sample, in agreement with the theoretical volume-temperature diagram for glass-forming liquids [18].

For the glass composition 25PbO–50MoO<sub>3</sub>–25P<sub>2</sub>O<sub>5</sub>, differential thermal analysis was used for the study of the dominant crystallization mechanism by the method of Ray and Day [19]. The crystallization mechanism (surface or internal) was evaluated from changes in the shape and position of the crystallization peak on DTA curves in the dependence on the particle size (120, 300, 600 and 900 μm) of the studied glasses. Changes in the shape of the crystallization peak with the changing particle size of glass powder are shown in Fig. 8. As can be seen from this figure, the shape of the crystallization peak changes substantially with changes in the particle size of the glass. It is obvious, that when increasing the grain size of the sample, the crystallization peak shifts to a higher temperature and its height is decreases, while the width of the peak increases. This behavior, according to [19], is typical for surface crystallization. These results suggest that the glass of the composition 25PbO–50MoO<sub>3</sub>–25P<sub>2</sub>O<sub>5</sub> nucleates predominantly via the surface crystallization mechanism,

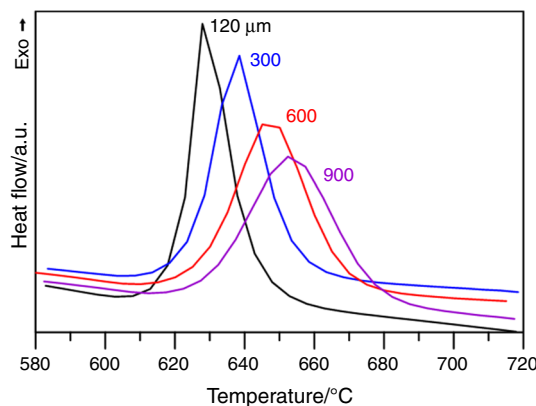


**Fig. 8** Change of the crystallization peaks for 25BaO–50MoO<sub>3</sub>–25P<sub>2</sub>O<sub>5</sub> glass depending on the grain size of the sample

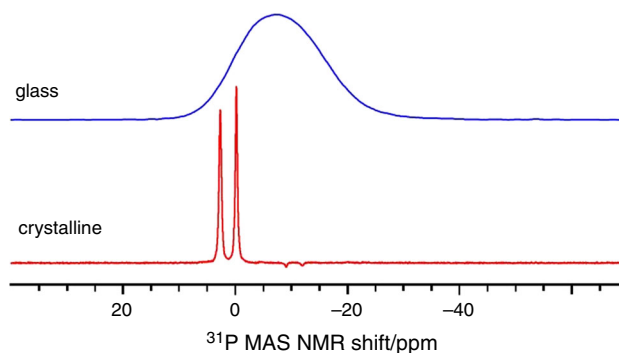


**Fig. 9** <sup>31</sup>P MAS NMR spectra of 25BaO–50MoO<sub>3</sub>–25P<sub>2</sub>O<sub>5</sub> glass and the corresponding polycrystalline compound Ba(MoO<sub>2</sub>)<sub>2</sub>(PO<sub>4</sub>)<sub>2</sub>

thereby producing crystalline compound Ba(MoO<sub>2</sub>)<sub>2</sub>(PO<sub>4</sub>)<sub>2</sub>.

We also measured <sup>31</sup>P MAS NMR spectra of 25BaO–50MoO<sub>3</sub>–25P<sub>2</sub>O<sub>5</sub> glass and the corresponding crystalline Ba(MoO<sub>2</sub>)<sub>2</sub>(PO<sub>4</sub>)<sub>2</sub> phase (see Fig. 9). As can be seen from this figure, the glass NMR spectrum represents a broad resonance band with a chemical shift of  $-7.3$  ppm (taken from the maxima of the resonance). On the other hand, the crystalline spectrum consists of two sharp resonances with a chemical shift value  $+2.6$  ppm and  $-0.3$  ppm, which indicates two environments of phosphorus atoms in the crystalline Ba(MoO<sub>2</sub>)<sub>2</sub>(PO<sub>4</sub>)<sub>2</sub> compound. A comparison of the Raman spectra of glass and crystalline samples is given in Fig. 10. A dominant vibrational band at  $954 \text{ cm}^{-1}$ , with a wide shoulder located on the left side of the main vibrational band, is ascribed to the presence of Mo–O bonds in the glass structure [20]. We believe that the band at  $954 \text{ cm}^{-1}$  should be ascribed to the terminal stretching vibration of MoO<sub>6</sub> polyhedra rather than only to the vibrations of M=O and M–O<sup>−</sup> bonds [4, 20].

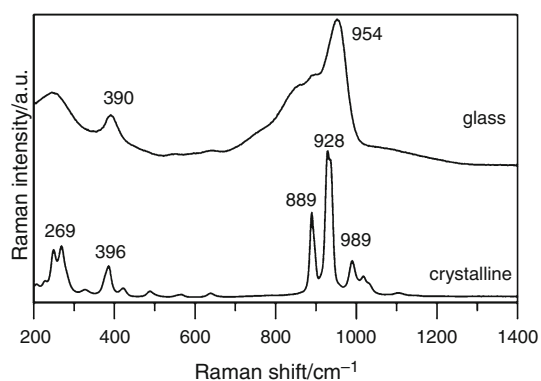


**Fig. 10** Raman spectra of 25BaO–50MoO<sub>3</sub>–25P<sub>2</sub>O<sub>5</sub> glass and the corresponding polycrystalline compound Ba(MoO<sub>2</sub>)<sub>2</sub>(PO<sub>4</sub>)<sub>2</sub>

## Conclusions

This study of BaO–MoO<sub>3</sub>–P<sub>2</sub>O<sub>5</sub> system glasses showed on a large glass-forming series A: (100 – x)Ba(PO<sub>3</sub>)<sub>2</sub>–xMoO<sub>3</sub> with a broad glass-forming range (0–70 mol% MoO<sub>3</sub>) and a shorter glass-forming range in series B: 50BaO–yMoO<sub>3</sub>–(50 – y)P<sub>2</sub>O<sub>5</sub> (0–15 mol% MoO<sub>3</sub>). The thermal study of these glasses revealed extraordinary thermal stability for the glass 35BaO–30MoO<sub>3</sub>–35P<sub>2</sub>O<sub>5</sub> in the first glass series. The course of the compositional dependence of glass transition temperature in glass series A is governed by two factors—cross-linking density and different bond strength of P–O and Mo–O bonds. Crystallization of glasses also revealed a new structure of the compound Ba(MoO<sub>2</sub>)<sub>2</sub>(PO<sub>4</sub>)<sub>2</sub> with X-ray data different from the previously reported compound of the same composition, but prepared by hydrothermal synthesis. It seems that there are two different modifications of the compound Ba(MoO<sub>2</sub>)<sub>2</sub>(PO<sub>4</sub>)<sub>2</sub>. XRD results and the results of Raman spectra studies of crystalline products, obtained by annealing glass powders, are in good agreement; moreover, Raman spectra reveal the existence of glass-crystalline samples.

**Acknowledgements** The authors are grateful for the NMR spectra measurement to Bertrand Revel from the University of Lille, France.

## References

1. van Wazer JR. Phosphorus and Its Compounds, vol. 1. New York: Interscience; 1958.
2. Brow RK. Review: the structure of simple phosphate glasses. *J Non-Cryst Solids*. 2000;263&264:1–28.

3. Koudelka L, Kalenda P, Mošner P, Montagne L, Revel B. Structure-property relationships in barium borophosphate glasses modified with niobium oxide. *J Non-Cryst Solids*. 2016;437:64–71.
4. Santagneli SH, de Araujo CC, Strojek W, Eckert H, Poirier G, Ribeiro SJL, Messaddeq Y. Structural studies of NaPO<sub>3</sub>–MoO<sub>3</sub> glasses by solid-state nuclear magnetic resonance and Raman spectroscopy. *J Phys Chem B*. 2007;111:101–9.
5. de Araujo CC, Strojek W, Zhang L, Eckert H, Poirier G, Ribeiro SJL, Messaddeq Y. Structural studies of NaPO<sub>3</sub>–WO<sub>3</sub> glasses by solid state NMR and Raman spectroscopy. *J Mater Chem*. 2006;16:3277–84.
6. Kitheri J. Non-isothermal crystallization in BaO–Fe<sub>2</sub>O<sub>3</sub>–P<sub>2</sub>O<sub>5</sub> glasses, A comparison with iron phosphate and Cs<sub>2</sub>O–Fe<sub>2</sub>O<sub>3</sub>–P<sub>2</sub>O<sub>5</sub> glasses. *J Therm Anal Calorim*. 2017;. <https://doi.org/10.1007/s10973-017-6361-x>.
7. Sinouh H, Bih L, Manoun B, Lazor P. Thermal analysis and crystallization of the glasses inside the BaO–SrO–TiO<sub>2</sub>–NaPO<sub>3</sub> system. *J Therm Anal Calorim*. 2017;128:883–90.
8. Poirier G, Ottoboni FS, Cassanjes FC, Remonte A, Messaddeq Y, Ribeiro SJL. Redox behavior of molybdenum and tungsten in phosphate glasses. *J Phys Chem B*. 2008;112:4481–7.
9. Koudelka L, Rösslerová I, Holubová J, Mošner P, Montagne L, Revel B. Structural study of PbO–MoO<sub>3</sub>–P<sub>2</sub>O<sub>5</sub> glasses by Raman and NMR spectroscopy. *J Non-Cryst Solids*. 2011;357:2816–21.
10. Rösslerová I, Koudelka L, Černošek Z, Mošner P, Beneš L. Thermal properties and crystallization of PbO–MoO<sub>3</sub>–P<sub>2</sub>O<sub>5</sub> glasses. *J Mater Sci*. 2011;46:6751–7.
11. Masse R, Averbuch-Pouchot MT, Durif A. Crystal structures of phosphomolybdate salts: Pb(MoO<sub>2</sub>)<sub>2</sub>(PO<sub>4</sub>)<sub>2</sub> and Ba(MoO<sub>2</sub>)<sub>2</sub>(PO<sub>4</sub>)<sub>2</sub>. *J Solid State Chem*. 1985;58:157–63.
12. Koudelka L, Kalenda P, Mošner P, Holubová J, Montagne L, Revel B. Structural study of BaO–MoO<sub>3</sub>–P<sub>2</sub>O<sub>5</sub> glasses by Raman and NMR spectroscopy. *J Non-Cryst Solids*. 2017;476:114–21.
13. Joint Committee on powder diffraction standards, Swarthmore, PA, USA. International Centre of Diffraction Data.
14. Lide DR. Handbook of Chemistry and Physics. Boca Raton: CRC Press; 2001. p. 9–52.
15. de Wolff PM. A simplified criterion for the reliability of a powder pattern indexing. *J Appl Crystallogr*. 1968;1:108–13.
16. Smoth GS, Snyder RL. A criterion for rating powder diffraction patterns and evaluating the reliability of powder-pattern indexing. *J Appl Crystallogr*. 1979;12:60–5.
17. Laugier J, Bochu B. LMGP-Suite, ENSP/Laboratoire des Matériaux et du Génie Physique, Saint Martin d’Heres, France, <http://www.inpg.fr/LMGP> and <http://www.ccp14.ac.uk/tutorial/lmgp/>. Accessed Dec 2007.
18. Varshneya AK. Fundamentals of Inorganic glasses. 2nd ed. Sheffield: The Society of Glass Technology; 2006. p. 19.
19. Ray CS, Day DE. Identifying internal and surface crystallization by differential thermal analysis for the glass-to-crystal transformations. *Thermochim Acta*. 1996;280–281:163–74.
20. Chowdari BVR, Tan KL, Chia WT, Gopalakrishnan R. Thermal, physical, electrical and XPS studies of the Li<sub>2</sub>O:P<sub>2</sub>O<sub>5</sub>:MoO<sub>3</sub> glass system. *J Non-Cryst Solids*. 1991;128:18–29.